

Perturbed biology and physics signatures in a 1-D ocean biogeochemical model ensemble

Article

Published Version

Creative Commons: Attribution 4.0 (CC-BY)

Open Access

Anugerahanti, P., Roy, S. and Haines, K. (2020) Perturbed biology and physics signatures in a 1-D ocean biogeochemical model ensemble. *Frontiers in Marine Science*, 7. 549. ISSN 2296-7745 doi: <https://doi.org/10.3389/fmars.2020.00549>
Available at <https://centaur.reading.ac.uk/91326/>

It is advisable to refer to the publisher's version if you intend to cite from the work. See [Guidance on citing](#).

To link to this article DOI: <http://dx.doi.org/10.3389/fmars.2020.00549>

Publisher: Frontiers

All outputs in CentAUR are protected by Intellectual Property Rights law, including copyright law. Copyright and IPR is retained by the creators or other copyright holders. Terms and conditions for use of this material are defined in the [End User Agreement](#).

www.reading.ac.uk/centaur

CentAUR

Central Archive at the University of Reading

Reading's research outputs online

Perturbed Biology and Physics signatures in a 1-D ocean biogeochemical model ensemble

Prima Anugerahanti,^{1,*}, Shovonlal Roy,^{1*} and Keith Haines,²

¹*Department of Geography and Environmental Science, University of Reading, Whiteknights, Reading, RG6 6AB, UK*

²*Department of Meteorology and National Centre for Earth Observation, University of Reading, Whiteknights campus Early Gate, Reading, RG6 6BB, UK*

Correspondence*:

Prima Anugerahanti

p.anugerahanti@pgr.reading.ac.uk

Shovonlal Roy

shovonlal.roy@reading.ac.uk

2 ABSTRACT

3 Sources of uncertainty in a marine biogeochemical model include input from physical processes
4 and the choice of functional forms representing the strength and dependencies of biogeochemical
5 processes. This study explores characteristic signatures from these uncertainties by generating
6 ensembles from perturbing the biogeochemistry equations and perturbing physical input using a
7 1-D intermediately-complex model run at five oceanographic stations. Perturbed biogeochemistry
8 ensemble (PBE) produces larger spreads than perturbed physics ensemble (PPE), and distinctly
9 different ensemble variations. Fractions of nitrogen in phytoplankton pool from observations show
10 a larger variability than in any single model-ensemble member, but the PBE spread generally
11 captures this variability, whereas the PPE spread does not. The results show that the PBE method
12 gives a more realistic representation of uncertainty than PPE in our 1D-model setup. Our method
13 needs to be tested in more complex models in order to understand its significance on larger
14 scales.

15 **Keywords:** Perturbed biogeochemistry ensemble, Ocean biogeochemical model, Ensemble modelling, Structural uncertainty,
16 perturbed physics ensemble

1 INTRODUCTION

17 Ocean biogeochemical (OBGC) models have been developed to understand how the ocean ecosystem
18 responds to the changes in both the physics and the biogeochemistry (Doney et al., 2012; Yool et al.,
19 2013; Butenschon et al., 2016). Key uncertainties that affect OBGC models include physical processes,
20 with vertical mixing and upwelling of nutrients often poorly known (Doney, 1999; Sinha et al., 2010;
21 Friedrichs et al., 2006), and the various choices for formulating the biological processes such as nutrient
22 uptake, zooplankton grazing, and plankton mortality (Gentleman et al., 2003; Anderson et al., 2010;
23 Adamson and Morozov, 2013). These biological processes are described by functional forms relating
24 them to concentrations of plankton and nutrients, as well as ambient temperature and light availability.
25 Different physical environments can strongly affect simulations of chlorophyll distribution through the
26 water column (Friedrichs et al., 2006), as well as regional distributions of phytoplankton functional types at

the surface ocean (Sinha et al., 2010). Spurious vertical velocities that can occur when assimilating physical ocean data into models can also raise nutrient concentrations in the upper water column (Subramanian and Palmer, 2017). Furthermore, when using different physical models, anthropogenic CO₂ uptake can vary between 25%-30% (Doney et al., 2004). The structure of an OBGC model, especially the choice of the functional representation of biogeochemical processes, strongly determine the model dynamics (Edwards and Yool, 2000; Fussmann and Blasius, 2005). For example, when the grazing function alone is altered from hyperbolic to sigmoidal (both of which are common in the literature) three times higher phytoplankton concentrations can be produced (Anderson et al., 2010). Impacts of altering mortality are shown in both uncoupled Nutrient-Phytoplankton-Zooplankton (NPZ) models (Steele and Henderson, 1992; Edwards and Yool, 2000) and coupled OBGC models (Yool et al., 2011). Choosing a linear mortality, can double the diatom biomass at high latitudes, compared to using other functions (Yool et al., 2011). So the uncertainties arising from both physical and biogeochemical formulations may contribute to discrepancies between the models and observations (Anderson, 2010; Allen et al., 2010).

One way of accounting for these multiple sources of uncertainty is to move away from deterministic simulations towards ensemble results which can be designed to deliver a probability distribution of outcomes. Perturbed physics ensembles have, for example been used to estimate the uncertainties of climate projections (Tinker et al., 2015; Subramanian and Palmer, 2017) or to forecast the climate probabilistically (Tebaldi and Knutti, 2007; Murphy et al., 2007). Ensembles are also regularly used to quantify uncertainties in data assimilation applications (Anderson, 2001; Moradkhani and Meskele, 2010; Roy et al., 2012) to allow weighting of model results compared with new observations.

Recently, Anugerahanti et al. (2018) has introduced an approach for generating an ensemble of an OBGC model by perturbing its core biogeochemistry processes. Here we extend the study of Anugerahanti et al. (2018), to decouple and compare the variability that may arise in an intermediately complex 1-D OBGC model from both biology and physics uncertainties, by generating three sets of ensembles perturbing: (i) the biogeochemistry, by altering the choice of functional forms (perturbed biogeochemistry ensemble, PBE), (ii) the physics, by adding noise to the vertical velocity, mixed layer depth (MLD) and therefore the vertical diffusivity coefficient, supplying nutrients to the surface layers (perturbed physics ensemble, PPE), and (iii) both the biogeochemistry and physics together (perturbed biogeochemistry and physics ensemble, PBPE). Since the OBGC model behaviour varies across different biogeographical provinces (Kriest et al., 2012), the ensemble is run at five monitored ocean sites ranging from coastal to oligotrophic regions. We quantify the variability generated by the perturbed ensembles, identifying and distinguishing the characteristics from the different biological and physical perturbations based on several biogeochemical property metrics. From these characteristics we can explore how the different perturbations may affect the model dynamics.

This paper is organised as follows: Brief description of the 1-D OBGC model, generating the ensembles, and the description of metrics are explained in section 2. The basic diagnostics of the ensembles which relate to the bulk properties of the model states, followed by the effect of perturbations in vertical distribution of chlorophyll are discussed in section 3.1. The different characteristic signatures of the PBE and PPE are described and discussed in section 3.2. Finally the conclusions of the study are in section 4.

2 METHODS

We use the Model of Ecosystem Dynamics, nutrient Utilisation, Sequestration, and Acidification (MEDUSA 1.0) (Yool et al., 2011). MEDUSA is an intermediately complex biogeochemical model that has two

phytoplankton types (diatoms and non-diatoms), two zooplankton types (mesozooplankton and microzooplankton), and three nutrients (dissolved inorganic nitrogen, silica, and iron), and uses nitrogen as the model currency. The 1-D version of this model is run in the Marine Model Optimisation Testbed (MarMOT-1.1) (Hemmings et al., 2015). The physical forcings, such as vertical velocity and solar radiation, are taken from the NEMO-FOAM output (Storkey et al., 2010), with output frequency every 5-days for all of the stations. NEMO-FOAM is a data assimilation product and therefore biases in well observed quantities are small, however for temperature and mixed layer depth (MLD) we introduce an additional bias correction to match the mean seasonal physical conditions observed at the stations. The vertical diffusivity coefficient is matched to the bias corrected MLD. Bias correction is done for all of the stations apart from station PAP where observational data are insufficient, so at PAP we use unadjusted NEMO-FOAM output. The MEDUSA ensembles are run from 1 January 1998 to 31 December 2007, with output produced everyday, at five different oceanographic stations; oligotrophic (represented by stations BATS (32°50'N, 64°10'W) and ALOHA (22°45'N, 158°00'W)), coastal (represented by stations Cariaco (10°30'N, 64°40'W) and L4 (50°15'N, 4°12.3'W)), and abyssal plain (represented by station PAP (49°N, 16.5°W)). Further information about running MEDUSA and a map of the station locations can be found in the Supplementary section 1.

83

85 2.1 Generating the ensembles

We generate the PBE by altering the equivalent functional forms for key biogeochemical processes. In the previous study (Anugerahanti et al., 2018) we used all possible functional form combinations, generally used in literature to describe four key processes; nutrient uptake, phytoplankton and zooplankton mortalities, and zooplankton grazing. The functional forms for phytoplankton nutrient uptake are Monod (U_h), which is the default function, exponential (U_e), sigmoidal (U_s), and trigonometric (U_t). For plankton mortalities, the default function is hyperbolic (denoted ζ_h for zooplankton and ρ_h for phytoplankton). Other functions available in MEDUSA are: linear (ζ_l, ρ_l), quadratic (ζ_q, ρ_q), and sigmoidal (ζ_s, ρ_s). Finally, for zooplankton grazing, we use Holling type III (G_1), which is the default function, and Holling type II (G_2). The shape defining parameters for these functional forms are tuned to each other so that over a wide range of conditions the key processes remains similar, see (Anugerahanti et al., 2018). Rate maxima are also similar to the original MEDUSA-1.0 run, apart from linear and quadratic mortalities, as these functions have no shape defining parameters. These process formulations with respective alternative functions made 128 combinations, which was the size of the original ensemble reported in Anugerahanti et al. (2018). But to reduce the computational cost while keeping the ensemble properties mostly unchanged, here we limit the biogeochemical ensemble to 12 members chosen using principal component analysis (PCA) and k-means cluster, to span a similar range of variability for measurable metrics of chlorophyll and nutrients as the larger ensemble (see Supplementary section 2, for further details).

At each of the stations the PPE is generated by adding “noise” to the vertical velocity, temperature, MLD and vertical diffusivity, in a regionally dependent and covarying way (as these fields are related) in order to increase variability, see supplementary section 3 for details. The vertical diffusivity profile is then matched to the perturbed MLD. The perturbations for vertical velocity at all stations are done by first subtracting the monthly average vertical velocity. The anomalies are multiplied by a random number between -2 and 2 and added to each five-day average field. These anomalies are generated randomly for each ensemble member. For station PAP, the perturbations to MLD are similar to perturbing the vertical velocity, and the vertical diffusivity profile is matched with the perturbed MLD. Further explanation of the PPE generation is in the Supplementary section 3, Figures S4 and S5. We use a PPE ensemble size of 12 members to match

the PBE ensembles discussed above. Finally the combination of perturbing physics and biogeochemistry together is generated by running the PBE using the physical inputs from the PPE, to produce a PBPE.

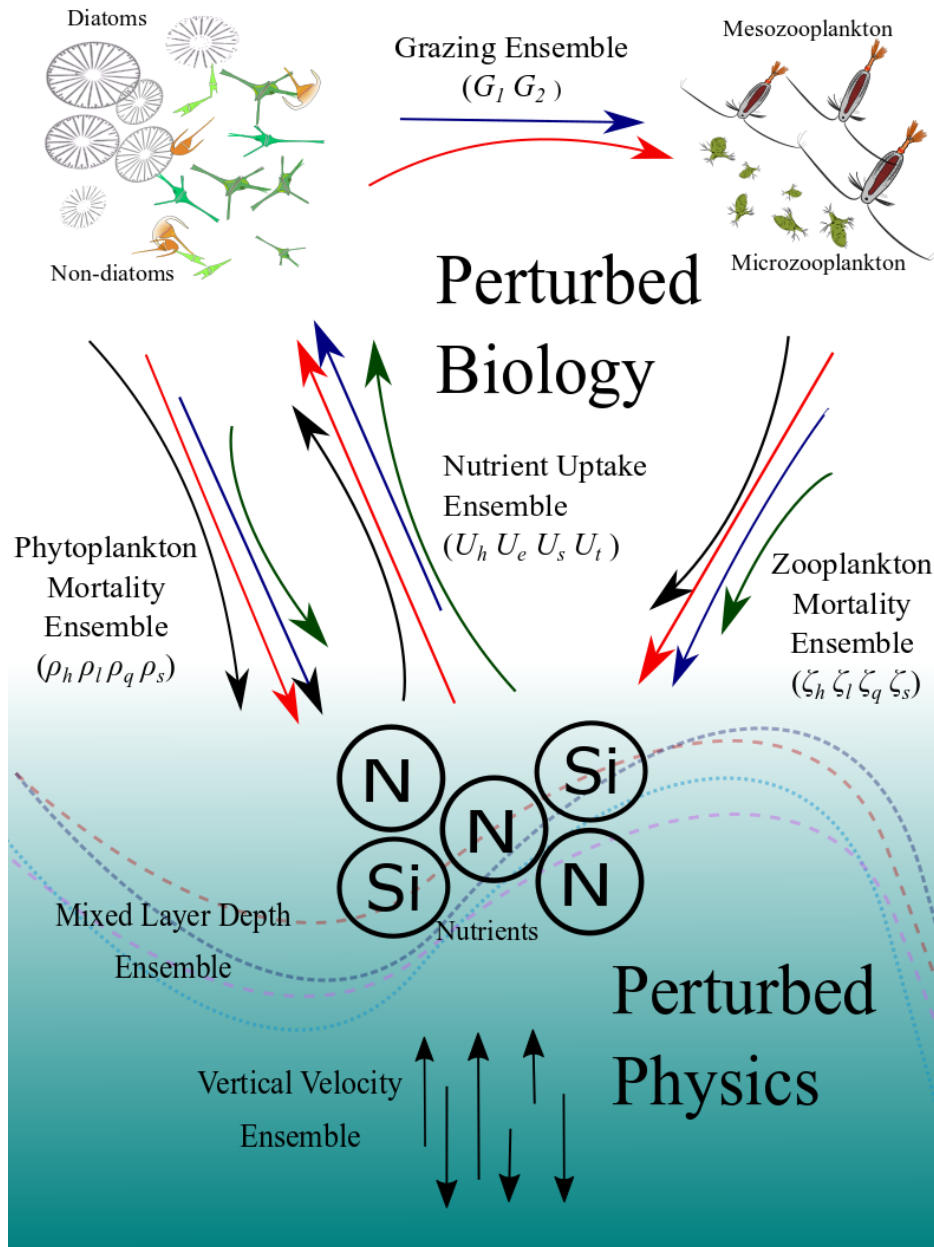


Figure 1. Schematic diagram showing how the ensembles are generated. The coloured and curved arrows in the top part represent the different functional forms which describe the key biogeochemical processes which generate the PBE. The straight vertical arrows at the bottom represent varying vertical velocities and the curved lines represent climatology of mixed-layer depths which generate the PPE. The PBPE is the combination of the two.

2.2 Ensemble metrics

We are interested in key properties of the model ensembles which we use to compare with observations at the five oceanographic stations. The spread of the annual means of dissolved inorganic nitrogen (DIN

mmol m⁻³), chlorophyll (mg m⁻³), and zooplankton (mmol m⁻³) concentrations are the basic diagnostics throughout the water column. At the oligotrophic stations a deep chlorophyll maximum (DCM) is a common feature that occurs below the mixed layer when surface chlorophyll concentration is low (Fennel and Boss, 2003; Letelier et al., 2004). The DCM evolution is explored phenologically by its maximum depth and concentration over the winter (December-January-February), spring (March-April-May), summer (June-July-August), and fall (September-October-November). The range of DCM depth, timing of maximum depth, and concentration are examined for both the PPE, PBE, and the observational data.

We also examine the fractions of total nitrogen in the phytoplankton pool to reveal a signature of the processes which have been varied within the ensembles, in particular this distinguishes PPE from PBE induced variations. This fraction is calculated by using the chlorophyll to nitrogen ratios, taken from Yool et al. (2011), for both the in situ and model ensemble. This metric can give an indication of the processes involved in the temporal changes seen from the in situ observations, suggesting it may be possible to infer which processes (physical, biological, or both) may be responsible for model-observational discrepancies at different times.

3 RESULTS

3.1 Chlorophyll Range and Distributions

Perturbations to the vertical velocity and MLD used for the PPE, produce relatively little spread in the bulk properties, especially for phytoplankton and zooplankton Figure 2. The PPE DIN concentrations vary little in the top 75m (in all stations except PAP), however the DIN range increases below, suggesting that the physical variations impact more below the euphotic layers. These deeper variations however do not have much impact on bulk properties near the surface such as the total DIN, chlorophyll (phytoplankton) or zooplankton concentrations (as seen in Figure 2). At the oligotrophic stations, the PPE range is clearly insufficient to cover the in situ concentrations. However at all five stations, from surface to deep water, the observed chlorophyll values mostly lie within the much larger PBE range (Figure 2a-d), suggesting that the full range of biological production through a strong nutrient gradient can be obtained by perturbing the biological processes. Only at the oligotrophic stations, below ~100m, are in situ chlorophyll concentrations still outside the PBE range. The combined PBPE ensemble has a slightly wider range than PBE but is otherwise similar.

The PBE and PPE members also differ in DCM generation at the oligotrophic stations. Figure 3 shows chlorophyll distributions from four different members at BATS and ALOHA, (see supplementary for monthly profiles of PPE section 5, Figures S8 to S11). The DCM is always present for part of each year but with considerable variability in maximum chlorophyll concentration and depth. In observations the deepest DCM always occurs in the summer and the shallowest in winter (Mignot et al., 2014). The range of DCM depths from the PBE is larger than that from the PPE, with observed deepest DCM depths generally within the PBE range (e.g. the deepest DCM depths at ALOHA, are 51-115m (PBE), 82-95m (PPE), and depth=114m from observations). Similarly, for the minimum DCM depth, the PBE produces a larger range, although this still underestimates that in the observations (PPE DCM range= 21-37m, PBE= 3-51m, observation=92m). Additionally all PPE members have the deepest DCM later in the autumn, instead of in summer, but not all PBE members show this discrepancy. There are some differences in chlorophyll distributions between PPE members and the default run, especially the thickness of the chlorophyll layer during winter/spring at BATS, although differences are not as distinct as for the PBE, as seen in Figure 3. The PBPE follows the pattern and timings of PBE, although the DCM depth range is slightly wider (e.g. at ALOHA, PBPE range 69-118m for maximum DCM depth).

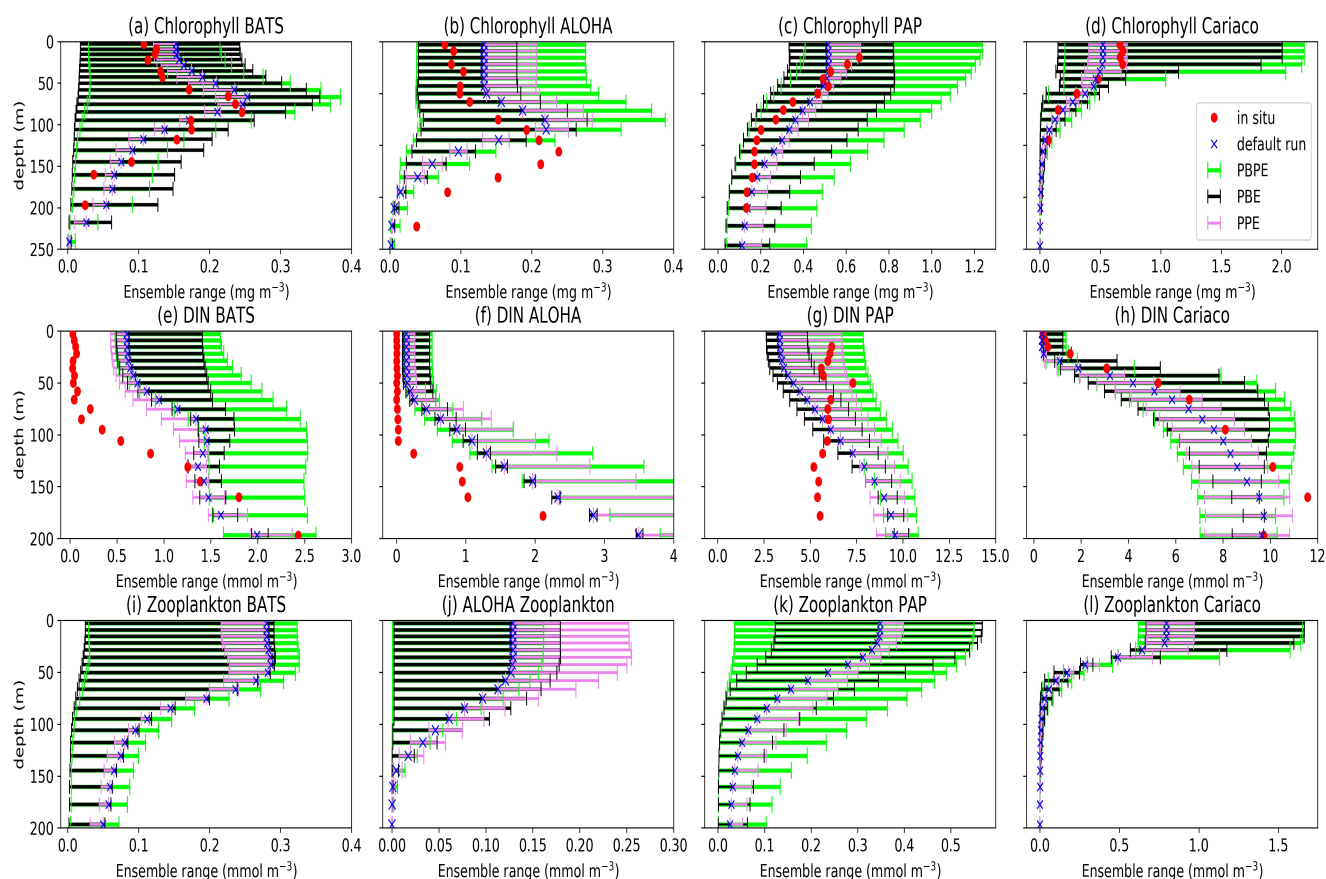


Figure 2. Ensemble range of mean chlorophyll (a to d), DIN (e to h), and zooplankton (i to l) profiles calculated from 1 January 1998- 31 December 2007 at BATS (a, e, and i), ALOHA (b, f, and j), PAP (c, g, and k), and Cariaco (d, h, and l). Blue crosses show the mean concentrations from the default run, red dots show the mean concentration from in situ, the violet bars denote the mean concentration from PPE, the green bars show the mean concentrations from the PBPE, and the black bars show the mean concentrations from the PBE. For station PAP the annual mean is taken between 2002 to 2004 for DIN and between 2003 to 2005 for chlorophyll (see Supplementary section 4, Figures S6 and S7, for the in situ monthly averages for DIN and chlorophyll at PAP). The model calculations for the annual means matched with the timing of observational sampling. Station L4 profiles are not shown because in situ data are only available at the surface.

159 These results suggest that perturbing the biogeochemistry can result in considerably greater variability in
 160 the evolution of the DCM, compared to perturbing the physics alone. Furthermore, when perturbing both
 161 physics and biogeochemistry, the effect of perturbing the latter predominantly determines the ensemble
 162 spread and chlorophyll distribution.

163 3.2 Characteristics of the different ensembles

165 The phytoplankton nitrogen fraction shows how much nitrogen resides in the phytoplankton pool, relative
 166 to the total DIN and phytoplankton nitrogen. The size of the phytoplankton nitrogen fraction can also
 167 indicate the concentration of nutrients (DIN) in the water column. For example, at ALOHA and BATS,
 168 the observed phytoplankton nitrogen fractions are always close to 1, indicating that most of the time, this
 169 region is nutrient limited. At stations such as L4, the phytoplankton nitrogen fraction can change drastically
 170 over the course of a season in both the observations and the model (Figure 4c and g).

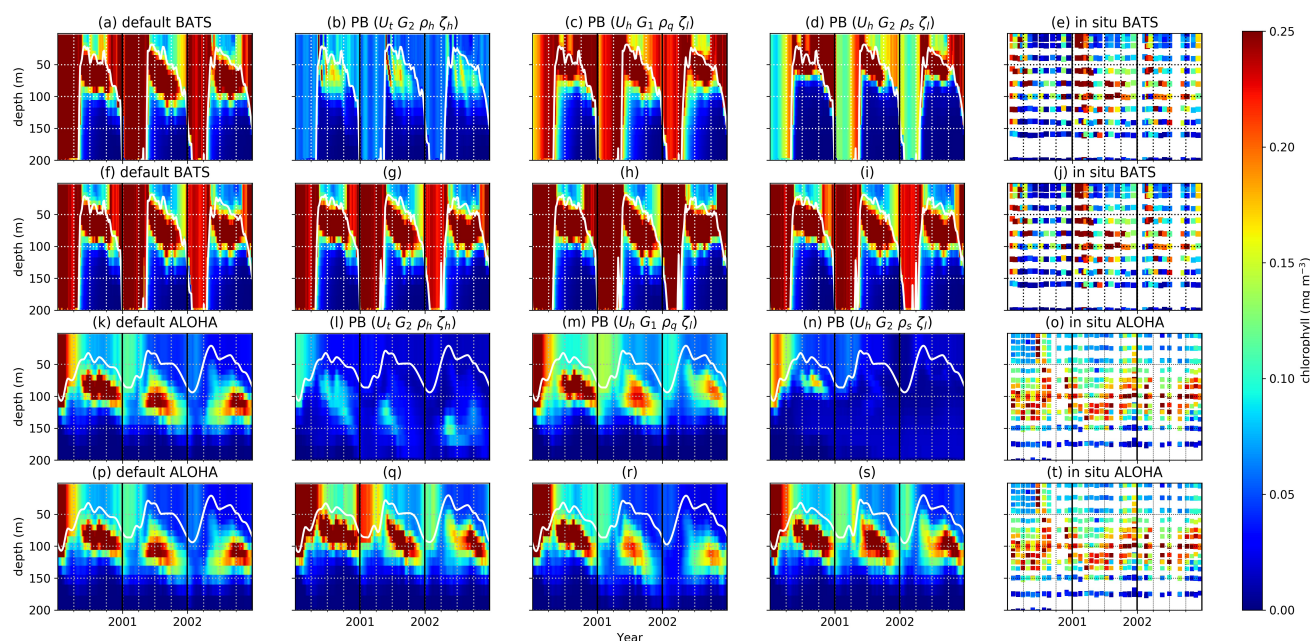


Figure 3. Chlorophyll distribution in the water column from 1st January 2000 to 31st December 2002 at station BATS (a to j) and ALOHA (k to t). White solid lines are the MLDs. Selected ensemble members, that are the most distinct from default run from PBE, with their functional form combinations are shown in (b) to (d), for BATS, and (k) to (n) for ALOHA, and for PPE are shown in (g) to (i) for BATS and (q) to (s) for ALOHA

From figure 4a and b, the proportion of nitrogen in phytoplankton is seen to vary strongly across the PBE members. In contrast the PPE shows very little spread in nitrogen fractions across the whole ensemble, Figure 4e and f. However, at the coastal stations L4 and Cariaco, there is more variability between PPE ensemble members, Figure 4g and h, and the timing of maximum phytoplankton nitrogen fraction varies across the ensemble.

The contrast between PBE and PPE is more distinct in the phytoplankton nitrogen fractions than in the spread differences in chlorophyll, for example seen in Figure 2, where the PPE chlorophyll range is seen to show more spread than the phytoplankton nitrogen fraction, especially in the oligotrophic regions. The small changes in the functional representation of uptake, grazing, and mortality curves in the PBE, represented by the exchange arrows in the upper part of Figure 1, can strongly alter the mean nitrogen distributions because they directly alter the cycling between biological pools. In contrast the PPE variability really only alters the supply of nutrients from deeper layers, represented by the lower part of Figure 1, and not the fluxes between the biological compartments and biological fractional distributions, hence the smaller PPE spreads in Fig 4e-h. The larger PBE spreads mostly capture the observed seasonal variations in nitrogen fractions e.g. at L4, where the PPE ensemble cannot, and thus PBE provides a better representation of uncertainty.

4 DISCUSSION

Previous studies such as Najjar et al. (2007), show that a simple biogeochemical model forced by different GCMs can produce large variability in dissolved organic matter both in the surface and at depth. Another study by Séférian et al. (2013) shows that atmosphere-ocean models differing in ocean subgrid physics

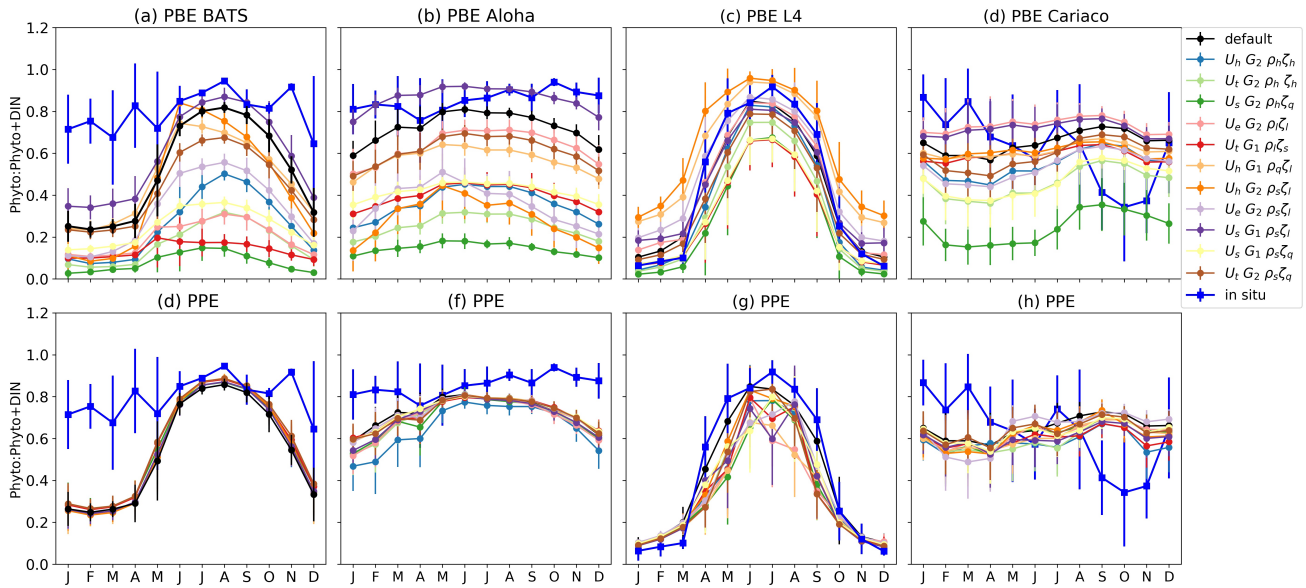


Figure 4. Monthly averaged phytoplankton fraction $P/(P+D)$ in nitrogen units at the surface for four oceanographic stations. The top and bottom panels show the phytoplankton fractions from PBE and PPE, respectively, with different lines representing ensemble members. The observations are shown in blue. The bars are the standard deviations of the monthly $P/(P+D)$. The nitrogen within phytoplankton is calculated using the chlorophyll to nitrogen ratio which is calculated using the C:N conversion fraction, and the calculation is described in Yool et al. (2011). These are calculated from 1 January 1998 to 31 December 2007, apart from station L4, which are calculated from January 2000, to match the in situ data.

190 and resolution can also produce varying biogeochemical tracers, such as nutrients and chlorophyll. In this
 191 study, we found that the uncertainty arising from biogeochemistry processes gives a larger range, especially
 192 in chlorophyll and zooplankton, as shown in Figures 2, and 4. In terms of bulk properties, the fact that a
 193 PPE generates a small range, is consistent with studies where different ocean general circulation models
 194 are coupled with the same OBGC model (e.g., Sinha et al. (2010)). However, below the depths of $\sim 75\text{m}$
 195 the PPE DIN shows a larger range, due to the absence of activities between nutrient phytoplankton and
 196 zooplankton, and physics perturbations therefore have more effect on DIN. At PAP the larger PPE DIN
 197 range, at depths of active phytoplankton growth may occur due to the restricted sampling to winter months,
 198 when biological activity is low even at the surface, and the physical perturbations are the only control on
 199 DIN.

200 Physically perturbing the vertical velocity, MLD, vertical diffusivity, and temperature in the PPE can alter
 201 the chlorophyll distributions in the water column and the depth of DCMs because these physical variables
 202 control the nutrients (vertical velocity and MLD) and light (MLD) availability (Siegel et al., 2002). The
 203 variations in nutrient and light availability then alter the timing of peak phytoplankton concentrations
 204 (Henson et al., 2013). Perturbing the MLD using the described method in supplementary section 3, changes
 205 the magnitude of vertical diffusivity leading to an increase/decrease in nutrient concentrations at euphotic
 206 depths (Huisman et al., 2006). From Figure 4 the PPE range depends on the model temperature bias; at
 207 stations where the model bias is small, such as BATS and ALOHA (mean temperature bias are -0.24 and
 208 -0.44 , respectively), the range of phytoplankton nitrogen fraction is low, and the seasonality is similar
 209 across members. However, at stations where model temperature bias is high, such as L4 and Cariaco (mean
 210 temperature bias are 0.90 and -1.58 , respectively), the PPE range is larger, with more variable seasonality.

Perturbing the biogeochemistry produces a larger range of DCM depths, as the DCM depends on nutrient uptake, zooplankton grazing, and plankton mortality from surface to deep water. This makes the depth of the DCM vary across all ensemble members when the grazing or mortality functions are altered (e.g. Figure 3b and g). The DCMs occur at depths where the phytoplankton growth rate is in balance with the loss rate (Fennel and Boss, 2003; Cullen, 2014). Variations in DCM depths, pattern, and continuity across the PBE are therefore due to different loss and growth rates throughout euphotic depths. In oligotrophic regions, the nutrient concentration is low in the top $\sim 150\text{m}$ (see Figure 2e and f). Some PBE members produce higher phytoplankton loss rates compared to growth rate in the top 75m due to the nutrient scarcity (e.g. members which use G_2 , ρ_h , and ρ_l). At deeper depths, nutrient is plentiful allowing phytoplankton growth to exceed the loss rate, giving a deeper DCM for these PBE members. When the mixed layer becomes deeper, a balance cannot be achieved as light becomes a limiting factor and chlorophyll concentrations reduce (see Figure 3b and g). The slightly larger maximum DCM depth range in PBPE may be caused by the additional net upwelling and the change in mixed layer depth from perturbing the physics, which gives the maximum depth for members with more downwelling and deeper MLD, and therefore a deeper DCM.

PBE and PPE ranges are also shown and compared for nitrogen fractions in Figure 4, because nitrogen is the model currency and we can examine its distribution to phytoplankton across different ensemble members, and these variables are available from observations. Variations in phytoplankton nitrogen proportions, both temporal and between the PPE members, may result from perturbing the MLD, as this can also controls the timing of maximum phytoplankton concentrations, by controlling the light and nutrient availability, as well as distribution of phytoplankton in the water column (Behrenfeld et al., 2013; Henson et al., 2013).

At station BATS, only three PBE members produce a nitrogen fraction comparable to that seen in the observations; the default function, $U_h G_2 \rho_s \zeta_l$, and $U_s G_1 \rho_s \zeta_l$. This is because the hyperbolic uptake function has higher nutrient uptake at low nutrient concentrations, compared to other functional forms, and both sigmoidal phytoplankton mortalities and linear zooplankton mortality produce lower phytoplankton loss. Note that the uptake functions in the default MEDUSA and the ensemble do not permit acclimatisation in nutrient uptake, such as described in Smith et al. (2009). The underestimation at the oligotrophic stations may also be caused by the bias introduced when reducing the ensemble members from 128 to 12 (see details in Supplementary section S2), which considers observations and model outputs at all stations across different oceanographic regions, in which there are 10 other PBE members that produce higher phytoplankton nitrogen fractions than the default run.

Apart from the possibility of inefficient uptake in the MEDUSA 1-D model, some physical parameters, such as horizontal advection and eddies, are not represented at all. In the subtropical gyre 3-D advection is thought to be essential in controlling primary productivity (Dave and Lozier, 2010; Palter et al., 2005), which may explain the discrepancies between the in situ and ensemble phytoplankton nitrogen fractions shown in Figure 4. In order to fully address the physical model bias, the impact of 3-D advection should be represented, and any errors in that circulation would need to be accounted for through ensemble spread, possibly by using multi-model ensembles, although even these may contain shared biases (Abramowitz et al., 2019).

Both PBE and PPE spreads are better at capturing the nitrogen fraction at light limited stations such as L4. The ensembles generally follow the observations, even when nutrients become limiting in the summer, because light also controls the nutrient uptake rate. The observed phytoplankton nitrogen fraction generally falls within the PBE range throughout the year, for example from October-March, the in situ phytoplankton fraction generally matches ensemble members with lower phytoplankton growth rates at

low concentrations (such as $U_t G_2 \rho_l \zeta_s$ and $U_h G_2 \rho_h \zeta_h$), and from April to September it matches members with higher phytoplankton growth rates and high zooplankton mortality (such as $U_h G_1 \rho_s \zeta_l$ and $U_h G_2 \rho_q \zeta_l$). This is consistent with North Atlantic bloom studies, where the phytoplankton nitrogen proportions and growth rates change over the year (Behrenfeld et al., 2013; Behrenfeld and Boss, 2014; Roy et al., 2012), being controlled by nutrients, light, and mixed layer conditions. For example in the summer, the growth rate of phytoplankton is in equilibrium with loss rate as nutrient is depleted and grazing rates are high (Behrenfeld et al., 2013; Behrenfeld and Boss, 2014).

These results suggest that in a 1-D biogeochemical model the PBE generates enough spread to encompass the uncertainty within the observed phytoplankton fraction even if the region is seasonally varying, and can explain the variations of growth and loss rate in phytoplankton. We can also see that none of the single PBE or PPE members fully capture the observations throughout the year, therefore using a single set of functional forms is not sufficient to capture the observed behaviour and its uncertainty. The PBE ensemble members that best match the in situ fractions vary through the year as the ensemble members behave differently depending on the concentrations of nutrient, phytoplankton, and zooplankton, especially in strongly seasonally varying regions.

We have further attempted to compare our PBE model with different biogeochemical model types used previously in model intercomparison studies e.g, Kwiatkowski et al. (2014). Acknowledging that the PBE model presented here was a 1D model, running only at 5 stations, a rigorous comparison with 3D models would be difficult. However, when compared to all surface observations at five stations, the mean of PBE surface chlorophyll produces a correlation of 0.55, with correlation range of [0.491, 0.583] produced by model ensemble members. In the inter-comparison study, Kwiatkowski et al. (2014) reported the range of [0.15, 0.50] across all models. Similarly, considering all observed surface DIN at five stations, the mean of PBE produces a correlation of 0.41, with the ensemble correlation range of [0.333, 0.595], which are lower than for the models reported by Kwiatkowski et al. (2014) which has surface DIN within the range [0.94, 0.79]. However, generality of the results needs to be tested beyond the five stations, and through comparison of other models with observations beyond annual average of surface fields.

When assessing the risks of climate change a structural ensemble may also be useful for representing model uncertainty. It has been shown in earlier studies, eg. by (Hawkins and Sutton, 2012) using a CMIP3 multimodel ensemble, that the uncertainty in climate change predictions may be strongly dominated by model uncertainty in the near term, and the detection time for anthropogenic impacts is conditioned by these uncertainties. The PBE ensemble method clearly demonstrates the importance of structural uncertainties, which should then be relevant in assessing climate change impacts on ecological indicators such as phytoplankton phenology.

5 SUMMARY AND CONCLUSION

We have run three different ensembles using 1-D MEDUSA, generated by perturbing the biology (PBE), the physics (PPE), and both together (PBPE). The ensemble spreads, chlorophyll distributions, and characteristics of these ensembles are explored. The PBE and PBPE generally produce larger spread of the chlorophyll annual means compared to PPE, and are able to encompass the in situ concentrations seen at 5 different oceanographic stations. Below the active phytoplankton growth region, the PPE produces larger DIN (nutrient) spread than PBE, as below this depth there is less biological activity and nutrient supply is dependent on the PPE. For the chlorophyll distributions we used the time evolution of the DCM as an ensemble metric at oligotrophic stations and this shows that across different ensemble members the PBE and PBPE produce larger spreads of DCM depth compared to PPE, with different chlorophyll

297 patterns. This is because the PBE produces more variable loss and growth rates of phytoplankton with
298 different nutrient supply rates. This means that perturbing the biogeochemistry produces a stronger effect
299 than perturbing physics.

300 To see how nitrogen, the model currency, is distributed to the phytoplankton compartments, we used
301 phytoplankton nitrogen fraction as a metric. This metric shows that the PBE produces a much larger spread
302 than PPE in terms of the monthly variability, and nearly covers the in situ standard deviations, especially at
303 the strongly seasonally varying stations. The large spread from the PBE show that altering the steepness
304 of the uptake, mortality, and grazing curves changes the way nitrogen is distributed to the phytoplankton
305 compartments, while in PPE the perturbations only alter the nutrient supply, both in terms of distribution in
306 the water column and concentrations.

307 Our 1D-model experiments suggest that the PBE or PBPE better represent model uncertainties arising
308 from the model structural errors, as shown by their ensemble ranges, and how the model currency is
309 distributed between the different compartments. A 1D model does however contain many simplifications
310 when it comes to ocean physics. To understand the implications of model structural errors on larger scales,
311 this method should also be tested in 3D coupled physical-biogeochemical models

ACKNOWLEDGEMENTS

312 The observation data for the oceanographic stations can be obtained from the following web-
313 sites; <http://hahana.soest.hawaii.edu/hot/hot-dogs/bextraction.html> for Sta-
314 tion ALOHA, <http://bats.bios.edu/bats-data/> for Station BATS, [http://imars.
315 marine.usf.edu/cariaco/biochemistry-microbiology-cruise-results](http://imars.marine.usf.edu/cariaco/biochemistry-microbiology-cruise-results) for Sta-
316 tion Cariaco, <https://www.westernchannelobservatory.org.uk/data.php> for Station
317 L4, and <http://projects.noc.ac.uk/pap/data> for Station PAP. The matlab code to derive
318 the mixed layer depth can be accessed in [https://uk.mathworks.com/matlabcentral/
319 fileexchange/53370-to-compute-mixed-layer-depth-based-on-subjective-method?
320 focused=5514769&tab=function](https://uk.mathworks.com/matlabcentral/fileexchange/53370-to-compute-mixed-layer-depth-based-on-subjective-method?focused=5514769&tab=function) The model output for this paper will be available in University
321 of Reading Research Data Archive, and can be accessed in [http://dx.doi.org/10.17864/1947.
322 214](http://dx.doi.org/10.17864/1947.214). This study was funded by the Bakrie Center Foundation (grant no. 1307/BCF-SK/RSCH/VII/2015)
323 and Yayasan Batavia Prosperindo Peduli (grant no. 005), Indonesia. The authors would like to thank Kevin
324 White, for his advice on this study, and John Hemmings, for providing the most recent version of the
325 MarMOT code.

CONFLICT OF INTEREST STATEMENT

326 The authors declare that the research was conducted in the absence of any commercial or financial
327 relationships that could be construed as a potential conflict of interest.

AUTHOR CONTRIBUTIONS

328 SR and KH conceived the study, and led the development of the methodology with PA. PA run the model,
329 performed the analysis, created visualisation and wrote the first draft of the manuscript. All authors
330 contributed significantly to writing the subsequent drafts and prepared the final version for publication.

REFERENCES

331 Abramowitz, G., Herger, N., Gutmann, E., Hammerling, D., Knutti, R., Leduc, M., et al. (2019).
332 ESD Reviews: Model dependence in multi-model climate ensembles: Weighting, sub-selection and
333 out-of-sample testing. doi:10.5194/esd-10-91-2019

- Adamson, M. W. and Morozov, A. Y. (2013). When can we trust our model predictions? Unearthing structural sensitivity in biological systems. *Proceedings of the Royal Society of London A: Mathematical, Physical and Engineering Sciences* 469, 20120500. doi:10.1098/rspa.2012.0500
- Allen, J. I., Aiken, J., Anderson, T. R., Buitenhuis, E., Cornell, S., Geider, R. J., et al. (2010). Marine ecosystem models for earth systems applications: The MarQUEST experience. *Journal of Marine Systems* 81, 19–33. doi:10.1016/j.jmarsys.2009.12.017
- Anderson, J. L. (2001). An Ensemble Adjustment Kalman Filter for Data Assimilation. *Monthly Weather Review* 129, 2884–2903. doi:10.1175/1520-0493(2001)129<2884:AEAKFF>2.0.CO;2
- Anderson, T. R. (2010). Progress in marine ecosystem modelling and the "unreasonable effectiveness of mathematics". *Journal of Marine Systems* 81, 4–11. doi:10.1016/j.jmarsys.2009.12.015
- Anderson, T. R., Gentleman, W. C., and Sinha, B. (2010). Influence of grazing formulations on the emergent properties of a complex ecosystem model in a global ocean general circulation model. *Progress in Oceanography* 87, 201–213. doi:10.1016/j.pocean.2010.06.003
- Anugerahanti, P., Roy, S., and Haines, K. (2018). A perturbed biogeochemistry model ensemble evaluated against in situ and satellite observations. *Biogeosciences* 15, 6685–6711. doi:10.5194/bg-15-6685-2018
- Behrenfeld, M. J. and Boss, E. S. (2014). Resurrecting the ecological underpinnings of ocean plankton blooms. *Annual review of marine science* 6, 167–94. doi:10.1146/annurev-marine-052913-021325
- Behrenfeld, M. J., Doney, S. C., Lima, I., Boss, E. S., and Siegel, D. A. (2013). Annual cycles of ecological disturbance and recovery underlying the subarctic Atlantic spring plankton bloom. *Global Biogeochemical Cycles* 27, 1291–1293. doi:10.1002/2013GB004681
- Butenschon, M., Clark, J., Aldridge, J. N., Icarus Allen, J., Artioli, Y., Blackford, J., et al. (2016). ERSEM 15.06: A generic model for marine biogeochemistry and the ecosystem dynamics of the lower trophic levels. *Geoscientific Model Development* 9, 1293–1339. doi:10.5194/gmd-9-1293-2016
- Cullen, J. J. (2014). Subsurface Chlorophyll Maximum Layers: Enduring Enigma or Mystery Solved? *Annual Review of Marine Science* 7, 207–239. doi:10.1146/annurev-marine-010213-135111
- Dave, A. C. and Lozier, M. S. (2010). Local stratification control of marine productivity in the subtropical North Pacific. *Journal of Geophysical Research: Oceans* 115, 1–16. doi:10.1029/2010JC006507
- de Boyer Montégut, C., Madec, G., Fischer, A. S., Lazar, A., and Iudicone, D. (2004). Mixed layer depth over the global ocean: An examination of profile data and a profile-based climatology. *Journal of Geophysical Research C: Oceans* 109, 1–20. doi:10.1029/2004JC002378
- Doney, S. C. (1999). Major challenges confronting marine biogeochemical modeling. *Global Biogeochemical Cycles* 13, 705–714
- Doney, S. C., Lindsay, K., Caldeira, K., Campin, J., Drange, H., Dutay, J., et al. (2004). Evaluating global ocean carbon models : The importance of realistic physics. *Global Biogeochemical Cycles* 18. doi:10.1029/2003GB002150
- Doney, S. C., Ruckelshaus, M., Emmett Duffy, J., Barry, J. P., Chan, F., English, C. A., et al. (2012). Climate Change Impacts on Marine Ecosystems. *Annual Review of Marine Science* 4, 11–37. doi:10.1146/annurev-marine-041911-111611
- Edwards, A. and Yool, A. (2000). The role of higher predation in plankton population models. *Journal of Plankton Research* 22, 1085–1112. doi:10.1093/plankt/22.6.1085
- Fennel, K. and Boss, E. (2003). Subsurface maxima of phytoplankton and chlorophyll: Steady-state solutions from a simple model. *Limnology and Oceanography* 48, 1521–1534. doi:10.4319/lo.2003.48.4.1521
- Friedrichs, M. A. M., Hood, R. R., and Wiggert, J. D. (2006). Ecosystem model complexity versus physical forcing: Quantification of their relative impact with assimilated Arabian Sea data. *Deep-Sea Research*

- 379 *Part II: Topical Studies in Oceanography* 53, 576–600. doi:10.1016/j.dsr2.2006.01.026
- 380 Fussmann, G. F. and Blasius, B. (2005). Community response to enrichment is highly sensitive to model
381 structure. *Biology letters* 1, 9–12. doi:10.1098/rsbl.2004.0246
- 382 Gentleman, W., Leising, A., Frost, B., Strom, S., and Murray, J. (2003). Functional responses for
383 zooplankton feeding on multiple resources: A review of assumptions and biological dynamics. *Deep-Sea*
384 *Research Part II: Topical Studies in Oceanography* 50, 2847–2875. doi:10.1016/j.dsr2.2003.07.001
- 385 Hawkins, E. and Sutton, R. (2012). Time of Emergence of climate signals. *Geophysical Research Letters*
386 38, 1–6. doi:10.1029/2011GL050087
- 387 Hemmings, J. C. P., Challenor, P. G., and Yool, A. (2015). Mechanistic site-based emulation of a global
388 ocean biogeochemical model (MEDUSA 1.0) for parametric analysis and calibration: An application of
389 the Marine Model Optimization Testbed (MarMOT 1.1). *Geoscientific Model Development* 8, 697–731.
390 doi:10.5194/gmd-8-697-2015
- 391 Henson, S., Cole, H., Beaulieu, C., and Yool, A. (2013). The impact of global warming on seasonality of
392 ocean primary production. *Biogeosciences* 10, 4357–4369. doi:10.5194/bg-10-4357-2013
- 393 Huisman, J., Pham Thi, N. N., Karl, D. M., and Sommeijer, B. (2006). Reduced mixing generates
394 oscillations and chaos in the oceanic deep chlorophyll maximum. *Nature* 439, 322–325. doi:10.1038/
395 nature04245
- 396 Kriest, I., Khatiwala, S., and Oschlies, A. (2010). Towards an assessment of simple global marine
397 biogeochemical models of different complexity. *Progress in Oceanography* 86, 337–360. doi:10.1016/j.
398 pocean.2010.05.002
- 399 Kriest, I., Oschlies, A., and Khatiwala, S. (2012). Sensitivity analysis of simple global marine
400 biogeochemical models. *Global Biogeochemical Cycles* 26, 1–15. doi:10.1029/2011GB004072
- 401 Kwiatkowski, L., Yool, A., Allen, J. I., Anderson, T. R., Barciela, R., Buitenhuis, E. T., et al. (2014).
402 IMarNet: An ocean biogeochemistry model intercomparison project within a common physical ocean
403 modelling framework. *Biogeosciences* 11, 7291–7304. doi:10.5194/bg-11-7291-2014
- 404 Letelier, R. M., Karl, D. M., Abbott, M. R., and Bidigare, R. R. (2004). Light driven seasonal patterns
405 of chlorophyll and nitrate in the lower euphotic zone of the North Pacific Subtropical Gyre. *Limnol.*
406 *Oceanogr* 49, 508–519. doi:10.4319/lo.2004.49.2.0508
- 407 Mignot, A., Claustre, H., Uitz, J., Poteau, A., Ortenzio, F. D., and Xing, X. (2014). Understanding the
408 seasonal dynamics and the deep chlorophyll maximum in oligotrophic. *AGU. global biogeochemical*
409 *cycles*, 856–876doi:10.1002/2013GB004781.Received
- 410 Moradkhani, H. and Meskele, T. T. (2010). Probabilistic Assessment of the Satellite Retrieval Error
411 Translation to Hydrologic Response. In *Satellite Rainfall Applications for Surface Hydrology*, eds.
412 M. Gebremichael and F. Hossain (Netherlands: Springer), chap. II. 235–241
- 413 Murphy, J. M., Booth, B. B. B., Collins, M., Harris, G. R., Sexton, D. M. H., and Webb, M. J. (2007). A
414 methodology for probabilistic predictions of regional climate change from perturbed physics ensembles.
415 *Philosophical transactions. Series A, Mathematical, physical, and engineering sciences* 365, 1993–2028.
416 doi:10.1098/rsta.2007.2077
- 417 Najjar, R. G., Jin, X., Louanchi, F., Aumont, O., Caldeira, K., Doney, S. C., et al. (2007). Impact
418 of circulation on export production, dissolved organic matter, and dissolved oxygen in the ocean:
419 Results from Phase II of the Ocean Carbon-cycle Model Intercomparison Project (OCMIP-2). *Global*
420 *Biogeochemical Cycles* 21. doi:10.1029/2006GB002857
- 421 Palter, J. B., Lozier, M. S., and Barber, R. T. (2005). The effect of advection on the nutrient reservoir in the
422 North Atlantic subtropical gyre. *Nature* 437, 687–692. doi:10.1038/nature03969

- Roy, S., Broomhead, D. S., Platt, T., Sathyendranath, S., and Ciavatta, S. (2012). Sequential variations of phytoplankton growth and mortality in an NPZ model: A remote-sensing-based assessment. *Journal of Marine Systems* 92, 16–29. doi:10.1016/j.jmarsys.2011.10.001
- Séférián, R., Bopp, L., Gehlen, M., Orr, J. C., Ethé, C., Cadule, P., et al. (2013). Skill assessment of three earth system models with common marine biogeochemistry. *Climate Dynamics* 40, 2549–2573. doi:10.1007/s00382-012-1362-8
- Siegel, D. A., Doney, S. C., and Yoder, J. A. (2002). The North Atlantic spring phytoplankton bloom and Sverdrup's critical depth hypothesis. *Science* 296, 730–3. doi:10.1126/science.1069174
- Sinha, B., Buitenhuis, E. T., Le Quere, C., and Anderson, T. R. (2010). Progress in Oceanography Comparison of the emergent behavior of a complex ecosystem model in two ocean general circulation models. *Progress in Oceanography* 84, 204–224. doi:10.1016/j.pocean.2009.10.003
- Smith, S., Yamanaka, Y., Pahlow, M., and Oschlies, A. (2009). Optimal uptake kinetics: physiological acclimation explains the pattern of nitrate uptake by phytoplankton in the ocean. *Marine Ecology Progress Series* 384, 1–12. doi:10.3354/meps08022
- Steele, J. H. and Henderson, E. W. (1992). The role of predation in plankton models. *Journal of Plankton Research* 14, 157–172. doi:10.1093/plankt/14.1.157
- [Dataset] Storkey, D., Blockley, E., Furner, R., Guiavarc'h, C., Lea, D., Martin, M., et al. (2010). Forecasting the ocean state using NEMO:The new FOAM system. doi:10.1080/1755876X.2010.11020109
- Subramanian, A. C. and Palmer, T. N. (2017). Ensemble superparameterization versus stochastic parameterization: A comparison of model uncertainty representation in tropical weather prediction. *Journal of Advances in Modeling Earth Systems* 9, 1231–1250. doi:10.1002/2016MS000857
- Tebaldi, C. and Knutti, R. (2007). The use of the multi-model ensemble in probabilistic climate projections. *Philosophical Transactions of the Royal Society A: Mathematical, Physical and Engineering Sciences* 365, 2053–2075. doi:10.1098/rsta.2007.2076
- Tinker, J., Lowe, J., Holt, J., Pardaens, A., and Wiltshire, A. (2015). Validation of an ensemble modelling system for climate projections for the northwest European shelf seas. *Progress in Oceanography* 138, 211–237. doi:10.1016/j.pocean.2015.07.002
- Yool, A., Popova, E. E., and Anderson, T. R. (2011). MEDUSA-1.0: A new intermediate complexity plankton ecosystem model for the global domain. *Geoscientific Model Development* 4, 381–417. doi:10.5194/gmd-4-381-2011
- Yool, A., Popova, E. E., and Anderson, T. R. (2013). MEDUSA-2.0: An intermediate complexity biogeochemical model of the marine carbon cycle for climate change and ocean acidification studies. *Geoscientific Model Development* 6, 1767–1811. doi:10.5194/gmd-6-1767-2013